



HAL
open science

Design of hyaluronan-based dopant for conductive biocompatible and resorbable PEDOT ink

Maxime Leprince, Pascal Mailley, Luc Choisnard, Rachel Auzély-Velty,
Isabelle Texier

► **To cite this version:**

Maxime Leprince, Pascal Mailley, Luc Choisnard, Rachel Auzély-Velty, Isabelle Texier. Design of hyaluronan-based dopant for conductive biocompatible and resorbable PEDOT ink. Carbohydrate Polymers, 2023, 301 Part B, pp.120345. 10.1016/j.carbpol.2022.120345 . cea-04248326

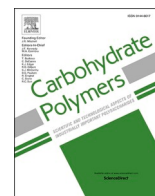
HAL Id: cea-04248326

<https://cea.hal.science/cea-04248326v1>

Submitted on 18 Oct 2023

HAL is a multi-disciplinary open access archive for the deposit and dissemination of scientific research documents, whether they are published or not. The documents may come from teaching and research institutions in France or abroad, or from public or private research centers.

L'archive ouverte pluridisciplinaire **HAL**, est destinée au dépôt et à la diffusion de documents scientifiques de niveau recherche, publiés ou non, émanant des établissements d'enseignement et de recherche français ou étrangers, des laboratoires publics ou privés.



Design of hyaluronan-based dopant for conductive and resorbable PEDOT ink

Maxime Leprince^{a,b}, Pascal Mailley^a, Luc Choisnard^c, Rachel Auzély-Velty^b, Isabelle Texier^{a,*}

^a Univ. Grenoble Alpes, CEA, LETI-DTBS, F-38000 Grenoble, France

^b Univ. Grenoble Alpes, CNRS, CERMAV, F-38000 Grenoble, France

^c Univ. Grenoble Alpes, CNRS, DPM, F-38000 Grenoble, France

ARTICLE INFO

Keywords:

Hyaluronan
PEDOT
Sulfation
Conductive ink
Degradable
Inkjet printing

ABSTRACT

Conformable biocompatible conductive materials are increasingly sought for the development of bioelectronics. If additionally resorbable, they could serve for the design of transient implantable electronic devices, opening the way to new healthcare applications. Hyaluronan (HA) derivatives including sulfate and aminophenylboronic acid (PBA) groups (HAS-PBA) were therefore designed to serve as dopants of poly(3,4-ethylenedioxy)thiophene (PEDOT). The optimized HA sulfation protocol allowed good control on polymer sulfation degree while minimizing polymer chain degradation. Sulfated HA was shown to be degradable in physiological conditions. A synergy was observed between the sulfate negative charges and the PBA aromatic groups promoting hydrophobic interactions and π -stacking between PEDOT and HAS-PBA, to boost the material conductivity that reached 1.6 ± 0.2 S/cm in physiological conditions. Moreover the PEDOT:HAS-PBA material was not cytotoxic and could be formulated for easy processing by inkjet printing, appearing as promising candidate for the design of soft transient electronics for in vivo applications.

1. Introduction

Bioelectronics, at the interface between living tissues and inert electronics, opens avenues in health monitoring, tissue stimulation, on-demand drug delivery, and electro-sensitive cell culture. Its rise relies on the development of soft flexible electronics (Someya et al., 2016; Wang et al., 2018), as living tissues are much softer and more flexible than traditional electronic materials (Liu et al., 2017). Though less efficient, conductive polymers can replace traditional conductors. Their mixed ionic/electronic conductivity is interesting for their use at the electronic/tissue interface as electric currents are supported by ionic flows in tissues, electron flows in electronic (Zozoulenko et al., 2021).

Among conductive polymers, poly(3,4-ethylenedioxy)thiophene (PEDOT) presents a good conductivity and compatibility with other materials, and noticeably a high biocompatibility (Kayser & Lipomi, 2019). PEDOT can be synthesized, usually in water, by the chemical oxidative polymerization of EDOT in the presence of a dopant, acting as a counter anion of the positively charged polymer. A colloidal suspension of PEDOT:dopant particles is therefore obtained, referred to as an ink. Ink particle size and conductive properties partly depend on the

polyelectrolyte dopant. Poly(styrene sulfonate) (PSS) is the most widely studied PEDOT dopant to design soft flexible conductive materials for bioelectronics (Kayser & Lipomi, 2019). PEDOT:PSS is commercially available at reasonable cost, presents tunable conductivity, thermal and chemical stabilities, and processability (Guo & Ma, 2018). However, its lack of biocompatibility and degradability led to the design of new conductive inks using biopolymers as dopants.

Several biomolecules have been investigated to obtain processable PEDOT:biomolecule inks: alginate (Xu, Cui, et al., 2019; Yang et al., 2020), dextran (Harman et al., 2015), pectin (Hofmann et al., 2017), xanthan (del Agua et al., 2018), deoxyribonucleic acid (DNA) (Tekoglu et al., 2020), heparin (Xu, Patsis, et al., 2019), chondroitin sulfate (ChS) or hyaluronic acid (HA) (Mantione et al., 2016; Wang et al., 2017). As they are resorbable, PEDOT:biomolecule composites can be used for the design of transient implantable electronic devices, that do not need invasive explantation when they have served their purpose (Boehler et al., 2019). To efficiently dope PEDOT, the selected polyanions must display acidic groups in the deprotonated form during EDOT polymerization (such as sulfates with $pK_a \approx 2$), to counter-balance the positive charges of the PEDOT domains (Hofmann et al., 2017). In order to

* Corresponding author.

E-mail addresses: pascal.mailley@cea.fr (P. Mailley), luc.choisnard@univ-grenoble-alpes.fr (L. Choisnard), rachel.auzely@cermav.cnrs.fr (R. Auzély-Velty), Isabelle.texier-nogues@cea.fr (I. Texier).

<https://doi.org/10.1016/j.carbpol.2022.120345>

Received 25 July 2022; Received in revised form 7 November 2022; Accepted 10 November 2022

Available online 15 November 2022

0144-8617/© 2022 Elsevier Ltd. All rights reserved.

increase PEDOT:biomolecule conductivity and to get closer to extracellular matrix structure, some of these biomolecules (dextran (Harman et al., 2015), cellulose (Horikawa et al., 2015) or alginate (Xu, Cui, et al., 2019)) were therefore sulfated. A PEDOT:dextran sulfate (DexS) ink presented a conductivity up to 7 S/cm and better interaction with L-929 cells than PEDOT:PSS (Harman et al., 2015). However, additional work highlighted that simply increasing the amount of dopant negative charges was not enough to increase the ink final conductivity. Sulfated cellulose (CellS) yielded more conductive ink than pristine cellulose (Cell), yet an optimal degree of sulfation was to be found (Horikawa et al., 2015). The electrical conductivity of PEDOT:CellS tended to increase with CellS crystallinity as PEDOT chains could line up around the rigid chains. Too sulfated CellS could hinder the crystallization process (Takano et al., 2012). Furthermore, rigid polyelectrolytes could yield to less doped and conductive PEDOT domains than more flexible ones (Gribkova et al., 2016a; Gribkova et al., 2016b). Additionally, because EDOT could interact with dopant hydrophobic moieties before polymerization, partly hydrophobic polyelectrolytes lead to the formation of more conductive PEDOT materials (Gribkova et al., 2016a, 2016b). All those considerations could explain why PEDOT:PSS is such a good conductive material.

Until now, the use of biomolecules to dope PEDOT has led to more biocompatible conductive inks than PEDOT:PSS, but to the detriment of conductivity. To the best of our knowledge, only DNA (Tekoglu et al., 2020) and DexS (Harman et al., 2015) based PEDOT inks have displayed conductivity >1 S/cm. Glycosaminoglycans (GAGs), namely hyaluronic

acid (HA), chondroitin sulfate (ChS) and heparin, led to highly biocompatible PEDOT:GAGs conductive materials, suitable for in-vivo recording and stimulation, but they all displayed low conductivity ($\sigma < 10^{-1}$ S/cm) (Mantione et al., 2016; Wang et al., 2017). Moreover, no correlation between the sulfation degree (DS_s) of these three GAGs and the conductivity of the resulting PEDOT:GAG films could be made. Additionally, only Harman et al. studied the processing of PEDOT:DexS ink by different techniques (drop casting, spray coating, inkjet printing, extrusion printing, laser etching) (Harman et al., 2015), whereas reported studies mainly analyzed ink characteristics after drop casting on glass slides only.

In this work, in order to design a resorbable biocompatible conductive ink, we selected hyaluronan as a building block. HA is a natural polysaccharide ubiquitous in the body and already widely used in various biomedical applications (Fallacara et al., 2018). As it is not sulfated in its pristine state, it is also appropriate to assess thoroughly the influence of dopant chemical modification on the final ink properties. We hypothesized that the introduction on HA backbone of sulfates (S) and aminophenylboronic acid (PBA) aromatic groups may “mimic” the PSS chemical functions (Fig. 1) and provide acidity, global negative charge, and hydrophobic π -stacking interactions with PEDOT, necessary to confer optimized conductivity to the inks. Therefore, we introduced in a controlled manner both sulfate and PBA moieties on HA, and the electrical, spectroscopic and biological properties of the obtained PEDOT:HA_{derivative} inks were systematically studied. We demonstrated that these materials were biocompatible and degradable in a few weeks

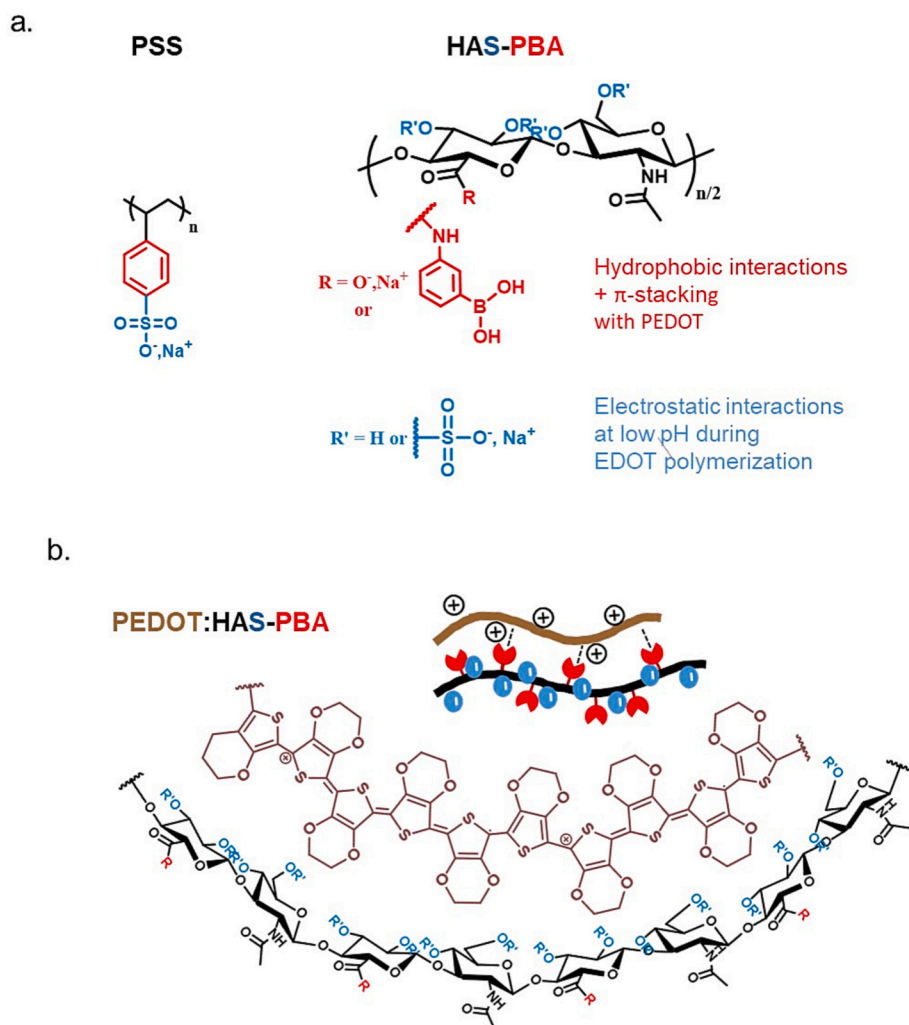


Fig. 1. Design of HAS-PBA derivatives mimicking PSS structure (a), to act as optimal dopants of PEDOT (b).

in physiological conditions, and could be easily processed by inkjet printing. To the extent of our knowledge, the systematic study of sulfation and the introduction of an aromatic group, as well as degradation properties, have never been reported before for a PEDOT:GAG ink or hydrogel, neither its processing by inkjet printing.

2. Materials & methods

2.1. Materials

Sodium hyaluronates of molar mass 113, 219, 478 kg/mol and of 1070 kg/mol were obtained from Lifecore Biomedical (Chaska, Minnesota, USA) and Kikkoman biochemifa company (Tokyo, Japan), respectively. Tetrabutylammonium hydroxide 30-hydrate (TBA-OH, (H₂O)₃₀), sulfur trioxide *N,N*-dimethylformamide (SO₃-DMF), ammonium persulfate (APS), 4-(4,6-dimethoxy-1,3,5-triazin-2-yl)-4-methylmorpholinium chloride (DMTMM), 3-aminophenylboronic acid hemisulfate salt (3APBA), dodecylbenzene sulfonic acid (DBSA), carbazole, sodium hydroxide pellets and WST-1 reagent (4-[3-(4-iodophenyl)-2-(4-nitro-phenyl)-2H-5-tetrazolio]-1,3-benzene sulfonate) were obtained from Sigma-Aldrich (Saint-Quentin Fallavier, France). 3,4-ethylenedioxythiophene (EDOT) and iron^{II} sulfate heptahydrate were from Alfa Aesar (Thermo Fisher GmbH, Kandel, Germany). Hydrochloric acid and glycerol were from Fischer Scientific (Fischer Scientific, Illkirch, France). *N,N*-dimethylformamide (DMF), ethanol 96 % (EtOH) and acetonitrile (MeCN) were from VWR International (Fontenay-sous-Bois, France). All reagents were used as received.

2.2. HA derivative synthesis protocols

2.2.1. HA sulfation

The sulfation protocol was adapted from the literature (Feng et al., 2017; Hintze et al., 2009; Kunze et al., 2010; Möller et al., 2012; Purcell et al., 2014). 1 g of HA was converted to tetrabutylammonium hyaluronate (HA-TBA) through elution on a H⁺-form ion exchange resin (Amberlite IR-130 from Sigma Aldrich), followed by addition of 0.4 M TBA-OH solution until pH 4.25 and freeze-drying. 1 g of HA-TBA was suspended in DMF at 4.7 g/L, then degassed and cooled down to 4 °C. *n* equivalents of SO₃-DMF dissolved in DMF at 123 g/L were added at once. The reaction medium was degassed and stirred for 1 h à 4 °C under nitrogen. The reaction was quenched by the addition of 667 mL of a NaOH solution containing (*n* + 1) equivalent of OH⁻ ions. The medium was neutralized, and NaCl was added to obtain a final NaCl concentration of 0.5 M. HAS was precipitated with 1.7 L of EtOH. Crude HAS was dissolved in 0.3 M NaCl and dialyzed against water with a dialysis membrane MWCO 6–8 kDa (Spectrum Laboratories, CA, USA) until bath conductivity was below 8 μS/cm, then recovered by freeze-drying with a yield of around 95 %.

2.2.2. Synthesis of HAS₄-PBA_{0,3}

The protocol was adapted from (Figueiredo et al., 2020). 1 g of HAS₄ was dissolved in 492 mL of water:DMF (3:2 v:v). One equivalent of DMTMM dissolved in 4 mL of water was added, then 0.3 equivalent of 3APBA dissolved in 4 mL of water. The pH was adjusted to 6.5 and the medium stirred overnight at room temperature. NaCl was added to obtain a final NaCl concentration of 0.3 M then, the product was purified by ultrafiltration on a 10 kDa ultra-filtration membrane (Amicon Bio-separations, Millipore, NH, USA). HAS-PBA was recovered after freeze-drying with a yield superior to 90 %.

2.3. NMR analysis

NMR spectra of the polysaccharide derivatives dissolved in deuterium oxide were recorded at 25 °C or 80 °C using a Bruker AVANCE III HD spectrometer operating at 400.13 MHz (¹H) and 100.61 MHz (¹³C). Detailed acquisition conditions, peak assignment and all NMR spectra

are reported in Supplementary Information.

¹H (D₂O, 80 °C) of HA-TBA: 4.68-4.36 (2H, dd), 4.25 (HOD signal), 3.95-3.25 (10H, m), 3.18-3.10 (8Ha, t), 2.10-1.84 (3H, s), 1.70-1.56 (8Hb, quint), 1.42-1.28 (8Hc, hex), 1.00-0.86 (12Hd, t).

¹H NMR (D₂O, 80 °C) of HAS: 5.04-4.9 (2H,m), 4.9-4.8 (1H, s), 4.68-4.58 (1H, d), 4.54-4.45 (2H, d), 4.42-3-4.33 (1H, t), 4.31-4.19 (HOD signal + 2H), 4.18-4.10 (1H, s), 3.99-3.91 (1H, m), 3.89-3.80 (1H, t), 2.27-2.06 (3H, s); ¹³C NMR (D₂O, 80 °C), 173.2, 103, 98.8, 77.2, 76.8, 75.7, 75.2, 75.0, 72.0, 66.5, 54.2, 21.7.

¹H NMR (D₂O, 80 °C) of HAS-PBA: 7.92-7.81 (0.3Ha, s), 7.70-7.53 (0.6Hb + c, dd), 7.50-7.40 (0.3H,d t), 5.08-3.56 (10H + HOD signal at 4.25, m), 2.32-1.94 (3H, s).

2.4. Measurement of HA sulfation degree

The sulfation degree, DS_S, defined as the mean amount of sulfate groups by HA repeating unit, was determined by chemical quantification (Supplementary Information) or elementary analysis. Elemental analysis was performed on a CHNS Flash EA1112Series analyzer (Thermo-Finnigan Inc.), heated at 950 °C in a quartz tube filled with copper and zinc oxide, and quartz wool for separation. Gases were carried by helium, separated at 54 °C in the chromatography column, and detected by a thermal conductivity detector.

2.5. Size exclusion chromatography (SEC)

The molar mass distribution and the weight-average molar mass of sulfated hyaluronic acids were determined by SEC using a Waters GPC Alliance chromatograph (Waters, Saint-Quentin-en-Yvelines, France) equipped with a differential refractometer and a light scattering detector (MALS) from Wyatt (Santa Barbara, USA). The solutions were injected at a concentration of 0.7 mg/mL in 0.1 M NaNO₃/0.005 M NaN₃, at a flow rate of 0.5 mL/min and at a column temperature of 30 °C. Samples and mobile phases were filtered under 0.1 μm before injection in the column. The variation of the refractive index according to the concentration (dn/dc) values of sulfated and pristine hyaluronic acid (sulfation degree of 2.1, 3.3 and 4) were determined with the same refractometer (0.05 and 0.40 g/mol concentration range).

2.6. Synthesis of PEDOT:HAS_x-PBA_y inks

The protocol was adapted from (Harman et al., 2015) with minor modifications. 1 g of HAS_x-PBA_y (0.5 eq) on one side, and 714 mg of APS (1.33 eq) on another side, were dissolved into degassed water (Section 3.4) or water:MeCN (9:1 v:v) (Sections 3.2–3.3). EDOT (251 μL, 334 mg, 1 eq) and FeSO₄ (0.05 eq or 0.015 eq), then APS solution, were added at once to the HAS_x-PBA_y solution. The solution was eventually mixed for 10 min at 25,000 rpm using an Ultra Turrax T-10 basic disperser with S 10 N-8G dispersing tool (Roth, Karlsruhe, Germany). EDOT polymerization took place at room temperature under nitrogen until pH was stable (1.4–1.5). The medium was dialyzed against deionized water with dialysis membrane MWCO 6–8 kDa (Spectrum Laboratories, California, USA), changing the bath until water conductivity was below 8 μS/cm. Then pH was adjusted to 7.4 and PEDOT:HAS_x-PBA_y was recovered by freeze-drying as a deep blue powder, with a yield superior to 80 %.

2.7. Ink deposition on glass slides and conductivity measurements

Freeze-dried PEDOT inks were dissolved in water at the desired concentration and the suspension strongly stirred for 10 min and sonicated for 30 s. 60 μL of suspension were deposited inside a 1 cm silicon ring on a glass slide washed with acetone and ethanol. The ink was dried at room temperature. Ink film thickness *h* was measured with a Dektak DXT profilometer (Bruker, Palaiseau, France). Film sheet resistivity *R*_{sheet} (Ω/□, the "□" is adimensionnal, but kept to not confuse sheet resistance from bulk resistance) was determined using a 4-point probe

from Ossila (Power Cord Type, Sheffield, England). Conductivity σ was calculated as $\sigma = 1/R_{sheet} \cdot c$ where c was a geometric corrector coefficient determined by the software and h the film thickness.

2.8. UV-visible absorbance measurements

Absorbance was measured from 300 to 2000 nm using a Cary 7000 Universal Measurement Spectrophotometer (Agilent, Santa Clara, USA), on ink films deposited on glass slides. All spectra were normalized by film thickness h .

2.9. Cytotoxicity

NIH3T3 murine fibroblasts were seeded in 96-well plates at a density of 4000 cells per well and incubated during 24 h at 37 °C with growth medium (Supplementary Information). After 24 h, growth medium was replaced with 200 μ L of fresh medium added with PEDOT:HAS₄-PBA_{0.3} ink or one of its precursors at desired concentration. After 24 h, the growth medium was removed and replaced with 100 μ L of fresh medium and 10 μ L of WST-1 reagent to perform cytotoxicity assay (Supplementary Information).

2.10. Degradation study

HA samples were incubated at 1 mg/mL at 37 °C for several weeks, in ammonium acetate buffer at pH 5 with and without hyaluronidase (1000 U/mL) from bovine testes. Then sample fractions were aliquoted at different times and analyzed by SEC-MALS as previously described.

2.11. Dynamic light scattering (DLS)

DLS measurements were performed on a Zeta sizer NanoZS from Malvern Instruments Ltd. (Worcestershire, England). Samples were diluted at 0.05 g/L in water and equilibrated at 25 °C. Measurements were performed in triplicate. $Z_{average}$ values were reported.

2.12. Inkjet printing

Ink formulations were prepared by dissolving ingredients

(lyophilized PEDOT:HAS_x-PBA_y, DBSA, glycerol) in water, adjusting pH to 7.4 with NaOH 0.1 M, filtering successively through 3 μ m and 1.2 μ m cellulose filters, vortexing, and sonication (30 s). Conductive lines (1–2 cm length, 25 μ m drop-to-drop spacing) were printed at 25 °C using a Dimatix Material Printer DMP-2831 from Fujifilm with 10 pL droplet size (\sim 25 V applied voltage to the printer 21 μ m diameter nozzles). After printing, tracks were dried overnight.

2.13. Scanning electron microscopy (SEM)

SEM pictures were obtained using a Merlin microscope from Zeiss (Fougères, France) equipped with a Gemini electron gun and a high efficiency SE2 detector. The electron gun firing voltage was set at 2 kV.

3. Results & discussion

3.1. Hyaluronan chemical modification

To mimic the PSS structure, HA hydroxyl functions were sulfated, and PBA aromatic groups were grafted onto HA carboxylate functions (Fig. 2). PBA was selected because of its acknowledged biocompatibility (Figueiredo et al., 2020).

3.1.1. HA sulfation

Two main sulfur trioxide complexes, SO₃-Py and SO₃-DMF, have been used as sulfating reagents. As pyridine is a stronger Lewis base than DMF, SO₃-Py was reported to achieve lower sulfation degree (DS_S) (0.2 < DS_S < 1.9) than SO₃-DMF (0.4 < DS_S < 3.5). Although sulfation conditions and purification procedures varied from one publication to another, all pointed out an important chain degradation after sulfation ($DP_{w_{final}}/DP_{w_{initial}} \leq 0.11$ for HA samples with molar masses M_w in the range 380–440 kg/mol (Feng et al., 2017; Purcell et al., 2014), $DP_{w_{final}}/DP_{w_{initial}} \leq 0.07$ for M_w around 1 million g/mol (Hintze et al., 2009; Kunze et al., 2010; Möller et al., 2012), where DP_w represents the polymerization degree).

Herein, a two-step sulfation protocol was optimized from the above-quoted literature. The first step (Fig. 2i) consisted in converting the HA sodium salt to the tetrabutylammonium salt (HA-TBA) by an ion exchange process in order to enhance its solubility in DMF. In the second step (Fig. 2ii), HA-TBA was reacted with SO₃-Py or SO₃-DMF using DMF

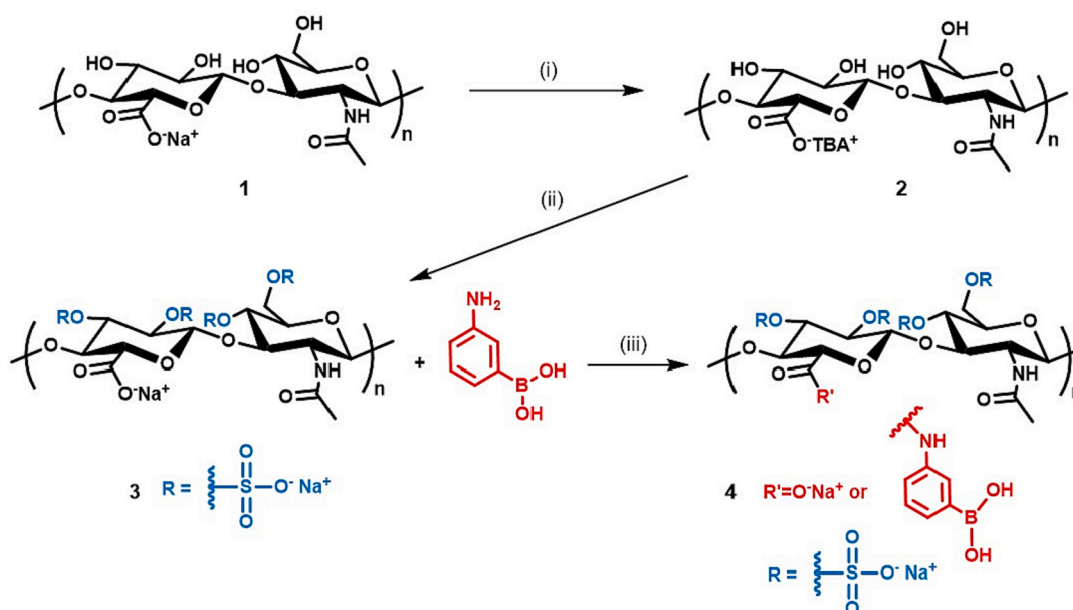


Fig. 2. Reaction scheme for the synthesis of sulfated HA derivatives bearing phenylboronic acid groups. Reagents and conditions: (i) Amberlite IR120 (H⁺) then, Bu₄NOH in H₂O; (ii) SO₃-DMF or SO₃-Py in DMF, then NaOH quenching and dialysis; (iii) DMTMM in H₂O/DMF, room temperature, 24 h.

as a solvent, followed by the introduction of an original basic quenching step after the sulfation reaction, to yield HAS (sulfation mass yield > 85 %).

Reaction studies were carried out starting from HA samples with different average molar mass (113, 219, 478, and 1070 kg/mol). The reaction time was set to 1 h because its increase resulted in more important chain degradation without significant increase of sulfation degree (Supplementary Information). Besides, HA sulfated at 30 °C was more degraded than when sulfated at 4 °C (Table 1, entries 1–2, 4–5, 8–9), because of reduced kinetics of HA hydrolysis at cold temperature. SO₃-Py yielded lower sulfation degree than SO₃-DMF (Table 1, entries 10–12, 11–13). Size exclusion chromatography (SEC-MALLS) showed that HAS prepared from HA samples with different molar masses exhibited a slight increase of polydispersity D (~10 %) in comparison to initial HA. No major degradation was observed for the derivatives prepared from HA with M_w of 113, 219, and 478 kg/mol ($DP_{w_{final}}/DP_{w_{initial}} > 0.40$ in most cases). On the other hand, the DP_w decrease was much more significant for the HAS derivatives prepared from HA with M_w 1070 kg/mol using SO₃-DMF, in agreement with the literature (Purcell et al., 2014).

To our knowledge, such high sulfation degree ($DS_S = 4$ for a classical amount of 20 eq. of SO₃-DMF) and such low chain degradation ($DP_{w_{final}}/DP_{w_{initial}} \sim 0.67$) is unprecedented. The increase of sulfation degree was attributed to the basic quenching of the sulfation reaction, neutralizing the formed sulfuric acid when water was added (Gilbert, 1962) (Fig. 2, step ii). As concentrated sulfuric acid can also be used as a polysaccharide de-sulfating agent, this could explain why literature protocols based on pure water quenching resulted in lower DS_S .

For the rest of this study, HA derivatives with initial M_w of 113 kg/mol, sulfated at 4 °C with SO₃-DMF, were selected since they displayed the minimum chain degradation during sulfation reaction ($DP_{w_{final}}/DP_{w_{initial}} \sim 0.7$).

3.1.2. Introduction of phenylboronic moieties

HAS with DS_S of 4 (entry 2, Table 1) and pristine HA were further modified to introduce PBA with a mass yield higher than 95 %. The amide coupling reaction between the carboxylic acid function of HAS and the amine function of 3APBA was conducted according to the conditions of (Figueiredo et al., 2020) (Fig. 2iii). The substitution degree in PBA (DS_{PBA}) was determined by ¹H NMR spectroscopy to be 0.3 (Supplementary Information). FTIR spectra of HA derivatives were also reported in Supplementary Information.

3.2. Synthesis and characterization of hyaluronan-based PEDOT inks

HA, HAS ($DS_S = 1.6, 3.0, 4.0$), HA-PBA ($DS_{PBA} = 0.3$) and HAS-PBA

($DS_{PBA} = 0.3, DS_S = 4.0$) were further used as dopants to prepare PEDOT inks. The oxidative chemical polymerization procedure was adapted from (Harman et al., 2015), with minor modifications. The HA derivatives and EDOT (EDOT/HA_{derivative} molar ratio = 2, one EDOT per saccharide unit) were dissolved in a mixture of water:MeCN (9:1, v:v) to improve EDOT solubility. Ammonium persulfate (APS) as oxidant, and Fe(SO₄) (0.05 eq.) as catalyst, were then added. Although 1.0 M equivalent of APS with respect to EDOT should be enough to achieve polymerization, 1.33 M equivalents were used to further oxidize PEDOT backbone, forming charge-propagating carriers. During polymerization, the reaction medium turned acid and deep blue (Fig. 3), and inks were recovered as deep blue powders.

X-ray photoelectron spectroscopy (XPS, Supplementary Information), Raman spectroscopy (Supplementary Information), ultraviolet to near-infrared spectroscopy, and 4-point probe conductivity measurements were performed on ink drop-casted films (5–15 μm thickness) on glass slides.

For all samples, the absorption band of neutral PEDOT (350–550 nm) was almost not present, as expected since 1.33 eq. of APS were added during polymerization to create charge carriers (Fig. 4a). For PEDOT:HAS_x, the intensity of charge carrier bands (radical cation and dications, displaying specific absorbance respectively around 800 nm and above 1000 nm (Gribkova et al., 2016a, 2016b; Zozoulenko et al., 2021)) increased as the DS_S increased. However PEDOT:HA-PBA_{0.3} exhibited higher absorption in the charge carrier bands. When both sulfate and PBA were present (PEDOT:HAS₄-PBA_{0.3}), charge carriers absorption bands were even more intense, evidencing a synergic effect between negatively charged sulfate and hydrophobic groups to efficiently dope the PEDOT chains.

PEDOT:HA displayed too low conductivity to be measured (Fig. 4b). For PEDOT:HAS_x, the macroscopic conductivity increased as the sulfation degree increased, from $3.2 \pm 0.7 \cdot 10^{-2}$ S/cm to $1.6 \pm 0.4 \cdot 10^{-1}$ S/cm. Interestingly PEDOT:HA-PBA_{0.3} displayed lower conductivity ($3.5 \pm 0.9 \cdot 10^{-3}$) than all PEDOT:HAS_x inks, whereas it was more intrinsically doped according to absorbance measurements (Fig. 4a). PEDOT:HAS₄-PBA_{0.3} presented an unprecedented conductivity for a PEDOT:GAG ink ($\sigma = 1.6 \pm 0.2$ S/cm, $R_{sheet} = 5 \cdot 10^4 \Omega/\square$), demonstrating again the synergy between the sulfate and aromatic groups.

To optimize conductive properties at the macroscopic scale, both charge carrier mobility and intra/interchain charge transport are involved. We introduced both sulfate groups and PBA moieties on HA to increase its acidity and global negative charge (as evidenced by zeta potential measurement reported in Supplementary Information), as well as its hydrophobic π -stacking interactions with PEDOT. The introduction of sulfate or PBA moieties alone resulted in almost no conductivity enhancement of PEDOT:HA_{derivative} ink (σ (PEDOT:HAS_x) = 0.032–0.16

Table 1
HA sulfation study.

Entry	M_{wi} (kg/mol)	Sulfating agent	Equivalent of sulfating agent/HA (n)	Reaction temperature	DS_S	$DP_{w_{final}}/DP_{w_{initial}}$	$D_{final}/D_{initial}$
1	113	SO ₃ -DMF	20	30 °C	4	0.23	1.01
2	113	SO ₃ -DMF	20	4 °C	4	0.77	1.01
3	113	SO ₃ -DMF	10	4 °C	2.2	0.68	1.01
4	219	SO ₃ -DMF	20	30 °C	4	0.11	1.08
5	219	SO ₃ -DMF	20	4 °C	4	0.51	1.17
6	219	SO ₃ -DMF	15	4 °C	3.3	0.41	1.08
7	219	SO ₃ -DMF	10	4 °C	1.6	0.64	1.08
8	478	SO ₃ -DMF	20	30 °C	4	0.06	1.04
9	478	SO ₃ -DMF	20	4 °C	4	0.38	1.04
10	478	SO ₃ -DMF	15	4 °C	3.3	0.25	1.15
11	478	SO ₃ -DMF	10	4 °C	1.6	0.48	1.15
12	478	SO ₃ -Py	15	4 °C	1.4	0.71	1.16
13	478	SO ₃ -Py	10	4 °C	1.2	0.64	1.13
14	1070	SO ₃ -DMF	13	4 °C	3	0.13	0.9
15	1070	SO ₃ -DMF	8	4 °C	2.2	0.11	0.92
16	1070	SO ₃ -Py	10	4 °C	1.5	0.56	1.01
17	1070	SO ₃ -Py	15	4 °C	1.8	0.33	0.98



Fig. 3. Reaction scheme (a) and solution color change (b) during EDOT polymerization in the presence of HA derivatives.

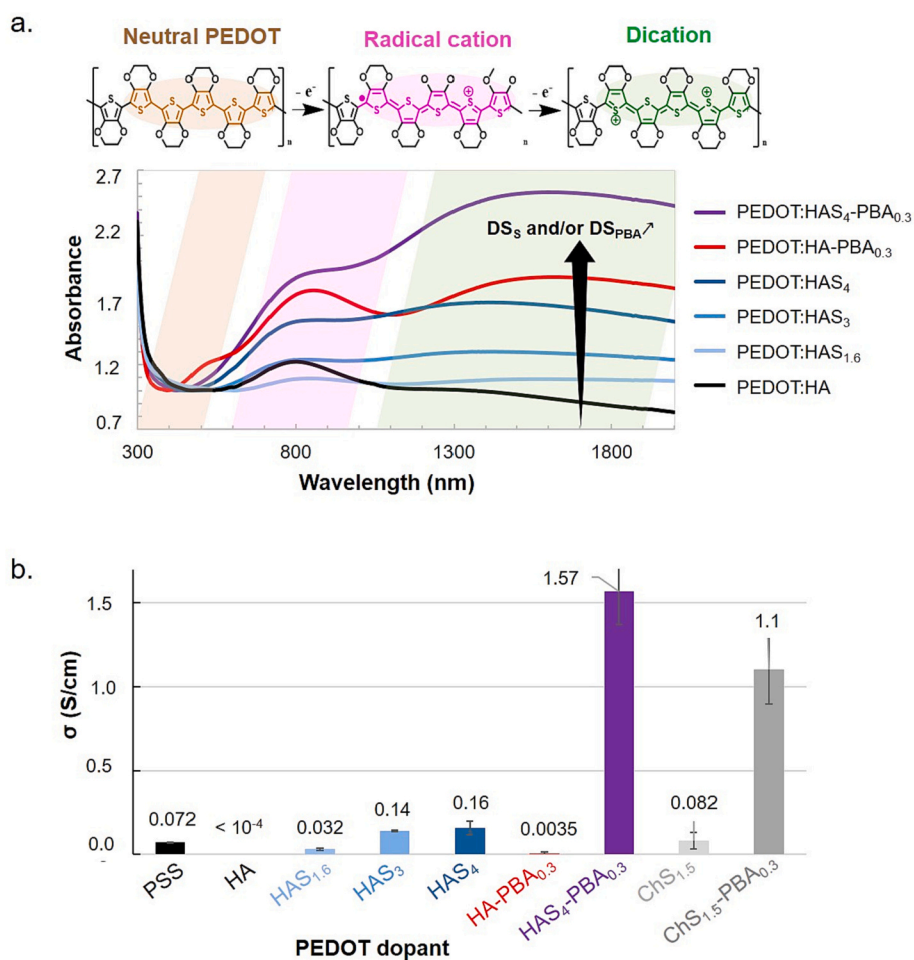


Fig. 4. Physico-chemical properties of PEDOT:HA_{derivative} inks drop-casted on glass slides: a) UV-visible-NIR absorption spectra (normalized according to film thickness); b) Conductivity measured by four-point probe (Values are compared to that of a commercial PEDOT:PSS ink (Clevios PH1000) prepared in PBS buffer at pH 7.4 and to prepared PEDOT:ChS_{derivatives}).

S/cm for $x = 1.6-4.0$, and σ (PEDOT:HA-PBA_{0.3}) = 0.0035 S/cm). In contrast, the simultaneous introduction of both sulfate and PBA resulted in a high increase of both the absorption in charge carrier bands and the conductivity, up to 1.57 S/cm. This synergy was also observed for another GAG, natural ChS (DS_S = 1.5). PEDOT:ChS_{1.5} ink displayed a conductivity of 0.082 S/cm, whereas it was 1.078 S/cm for PEDOT:ChS_{1.5}-PBA_{0.3}, showing again a synergistic effect of sulfate and PBA

(synthesis described in Supplementary Information). This synergistic effect was attributed to PEDOT/polyelectrolyte interactions: hydrophobic moieties in GAG-PBA_{0.3} enabled close association of PEDOT oligomers with polysaccharide backbone, resulting in stable radical cations and dications, as evidenced by spectrophotometry (Fig. 4a). However, because of the absence of sulfate groups along the polyelectrolyte, they could not efficiently propagate, resulting in a low

conductivity. By contrast, the numerous sulfate groups in the ChS or HAS_x samples enabled charge propagation all along the PEDOT oligomers associated to the polysaccharide chains, but did not create high charge carrier concentration in PEDOT domains. For HAS₄-PBA_{0.3} or ChS-PBA_{0.3}, hydrophobic moieties enhanced charge carrier concentrations, and negative sulfated charges enabled their propagation. Noticeably, PEDOT:HAS₄-PBA_{0.3} ink displayed better conductive properties than PEDOT:PSS in physiological conditions ($7.2 \pm 1.3 \cdot 10^{-2}$ S/cm for Clevis PH1000 films deposited on a glass slide at pH \approx 7.4 in PBS), without secondary doping. To the best of our knowledge, the introduction of aromatic moieties on biomolecules to design new PEDOT bi-dopants has never been described. This work highlights the potential of this strategy.

3.3. Biological properties of PEDOT:HAS₄-PBA_{0.3} ink

3.3.1. Cytotoxicity

The cytotoxicity of PEDOT:HAS₄-PBA_{0.3} was assessed using a cell proliferation and viability WST-1 assay. A high viability of cells incubated with the ink was observed at all concentrations ($IC_{50} > 750$ μ g/mL, IC_{50} being the dose of cytotoxic compound at which 50 % mortality is achieved) (Supplementary Information). On an indicative basis, PEDOT:PSS IC_{50} value was reported to be below 1000 μ g/mL (Baek et al., 2014).

3.3.2. Degradability

HAS₄ degradation with or without hyaluronidase (HAase) was monitored over time using SEC-MALS to measure the chain average molar mass, and compared to that of HA (Fig. 5). Unfortunately, it was not possible to include HAS₄-PBA_{0.3} or PEDOT:HAS₄-PBA_{0.3} in the experiments, because of the interactions of PBA or PEDOT moieties with the chromatography column. Interestingly, HAS₄ (Fig. 5) but also HAS_{2.2} (data not shown) displayed the same degradation behavior, regardless HAase presence and concentration. They were degraded by roughly 40 \pm 10 % ($DPW_{final}/DPW_{initial} \sim 0.6$) and 70 \pm 10 % ($DPW_{final}/DPW_{initial} \sim 0.3$) in respectively two weeks and three months. The degradation rate of HAS₄ (with/without HAase) was more important than the degradation of HA alone (18 % in 3 months, $DPW_{final}/DPW_{initial} \sim 0.82$), but less important than the degradation of HA with HAase ($DPW_{final}/DPW_{initial} < 0.02$ in 24 h).

Sulfated HA therefore appeared degradable by auto-hydrolysis that cleaved the polymer chain into smaller oligomers, but not biodegradable, as the degradation rate was not linked to enzymatic activity. Regarding the lack of degradation of HAS by HAase, the sulfate groups could prevent the HAase/HA complex to form properly as the enzyme needs an available unmodified HA octasaccharide substrate to bind and cleave the polymer (Deschrevel et al., 2008). HAS fastened hydrolysis in comparison to HA could be attributed to the sulfate groups contributing to the hydrolytic auto-cleavage of the β 1,4-glucosaminidic bonds

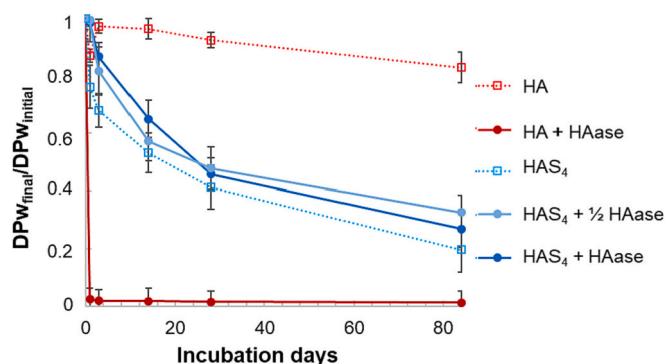


Fig. 5. Degradation of HA and HAS₄ at 37 °C in ammonium acetate 5 mM pH 5 with or without 1000 U/mL of hyaluronidase (500 U/mL for 1/2 HAase).

between glucosamine and glucuronic acid moieties, as it was observed in other sulfated polysaccharides such as carrageenan (Cosenza et al., 2016). Importantly, HAS₄ slowly hydrolyzed in physiological conditions. Probably HAS₄-PBA_{0.3} could do the same, as the low degree of PBA substitution should not modify hydrolysis mechanism.

3.4. Inkjet printing of HAS₄-PBA_{0.3}:PEDOT

With PEDOT:HAS₄-PBA_{0.3} material in hand, a formulation fully processable for bioelectronic device microfabrication was developed. Due to the water-flowing like behavior of PEDOT:HAS₄-PBA_{0.3} dispersion, inkjet printing was explored. Dimatix DMP-2800 drop-on-demand printer was selected since fully configurable and enabling to work with small volumes (0.5–2 mL). Ink optimal physicochemical specifications for this printer are: i) ink particle size below 1/10th of nozzle diameter (i. e. 2 μ m) to avoid clogging; ii) viscosity between 10 and 12 mPa·s; iii) surface tension between 28 and 33 mN/m.

With previously described protocol (Section 3.2), ink particle sizes above 1–3 μ m diameter with high polydispersity index (PDI > 0.4) were measured by Dynamic Light Scattering (DLS) at the end of EDOT polymerization. A homogenization step was therefore introduced at the very beginning of the polymerization to obtain inks composed of small monodisperse droplets. Optimized PEDOT:HAS₄-PBA_{0.3} formulation for inkjet printing was ink concentration of 30–35 g/L, in the presence of 2 g/L of dodecylbenzene sulfonic acid (DBSA) and 2.3 % vol. of glycerol to tend to viscosity and surface tension specifications (Supplementary Information). PEDOT:HAS₄-PBA_{0.3} ink particles of 767 ± 27 nm were obtained, with a film resistivity of 0.5–1 10^3 Ω/\square when drop-casted on glass slide.

Tracks (lines) were then printed on soft poly(urethane) (PU) films (Fig. 6a). The film resistivity decreased with the number of printed layers (from $8.0 \pm 1.0 \cdot 10^6$ to $4.1 \pm 0.3 \cdot 10^5$ Ω/\square for respectively 5 and 60 printed layers), as expected when track thickness increased. However, it resulted in a lowered printing resolution (track effective width of 500 μ m for 50 layers, for a printer value set at 160 μ m) (Fig. 6a, b), showing that successive ink layers flowed on each other. The structure of printed tracks was further analyzed by scanning electron microscopy (SEM) (Fig. 6b). Zoomed picture displayed some granularity, in accordance with DLS measurements (767 nm diameter).

Usually, PEDOT:biomolecules inks are processed by electrospinning (Kiristi et al., 2013), drop casting (Mantione et al., 2016; Wang et al., 2017), spin coating or extrusion printing (Harman et al., 2015). Beforehand, only Harman et al. (2015) have reported inkjet printing of a PEDOT:DexS ink. Noticeably, they did not report the conductivity of the printed tracks. Herein, a sheet resistivity of 410 ± 30 k Ω/\square was obtained for 60 layers of printed PEDOT:HAS₄-PBA_{0.3} ink. To the best of our knowledge, the only work reporting the conductivity of printed PEDOT:PSS tracks without secondary doping or other treatments is the publication of Mire et al. (2011) in which commercial PEDOT:PSS was printed on a soft chitosan-HA film. The tracks were 40 μ m wide and 1.2 μ m thick with a conductivity of 0.7 S/cm, corresponding to a 2 cm long track resistance of \approx 400 k Ω , in the same range than PEDOT:HAS₄-PBA_{0.3} ink, which appears competitive.

4. Conclusions

We designed HAS-PBA as PEDOT dopant based on the hypothesis that the introduction on the HA backbone of sulfates and aromatic groups may “mimic” the chemical functions of PSS. We demonstrated that HAS-PBA provided acidity, global negative charge, and hydrophobic and π -stacking interactions with PEDOT, necessary to obtain conductive PEDOT:HAS-PBA inks. Additionally, we showed that there exists a synergy effect between the sulfate and the PBA aromatic groups to promote ink conductivity. PEDOT:HAS-PBA inks proved to be biocompatible, probably resorbable, and importantly easily processable. Once cross-linked to make them non water-soluble, they will display all

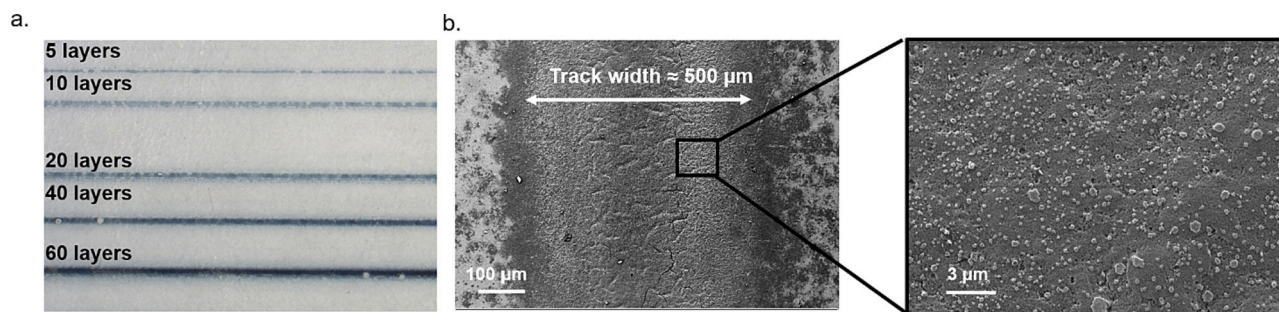


Fig. 6. Inkjet-printed tracks (5 mm long, 160 μm width) of PEDOT:HAS₄-PBA_{0.3} ink. a. Optical images of tracks on a poly(urethane) film; b. SEM images of printed tracks (50 layers) on a silicon substrate.

necessary hallmarks for the design of transient bioelectronics devices.

CRedit authorship contribution statement

Maxime Leprince: Investigation, Writing – original draft. **Pascal Mailley:** Conceptualization, Writing – review & editing. **Luc Choinard:** Methodology. **Rachel Auzély-Velty:** Conceptualization, Validation, Writing – review & editing, Supervision. **Isabelle Texier:** Conceptualization, Validation, Writing – original draft, Writing – review & editing, Supervision.

Declaration of competing interest

The authors declare that they have no known competing financial interests or personal relationships that could have appeared to influence the work reported in this paper.

Data availability

Data will be made available on request.

Acknowledgements

This work was supported by the French National Research Agency (ANR) in the framework of the STRETCH project (ANR-8-CE19-0018-01). LETI-DTBS and CERMAV are supported by ANR in the framework of the LabEx Arcane (grant ANR-17-EURE-0003) and Glyco@Alps (ANR-15-IDEX-02) programs. We greatly acknowledge the help of Mathilde Menneteau (CEA Grenoble/LETI/DTBS) for cytotoxicity, Sonia Ortega (CERMAV-CNRS) for SEC analysis, I. Jeacomine (CERMAV-CNRS) for her support at the NMR platform of ICMG (FR2607), and Yohann Thomas and Simon Régál (CEA Grenoble/LETI/DTBS) for SEM photographs.

Appendix A. Supplementary data

Supplementary data to this article can be found online at <https://doi.org/10.1016/j.carbpol.2022.120345>.

References

- Baek, S., Green, R. A., & Poole-Warren, L. A. (2014). Effects of dopants on the biomechanical properties of conducting polymer films on platinum electrodes. *Journal of Biomedical Materials Research Part A*, 102(8), 2743–2754.
- Boehler, C., Agrawala, Z., & Asplund, M. (2019). Applications of PEDOT in bioelectronic medicine. *Bioelectronics in Medicine*, 2(2), 89–99.
- Cosenza, V. A., Navarro, D. A., & Stortz, C. A. (2016). DFT/PCM theoretical study of the conversion of methyl 4-O-methyl- α -D-galactopyranoside 6-sulfate and its 2-sulfated derivative into their 3,6-anhydro counterparts. *Carbohydrate Research*, 426, 15–25.
- del Agua, I., Marina, S., Pitsalidis, C., Mantione, D., Ferro, M., Iandolo, D., Sanchez-Sanchez, A., Malliaras, G. G., Owens, R. M., & Mecerreyes, D. (2018). Conducting polymer scaffolds based on poly(3,4-ethylenedioxythiophene) and xanthan gum for live-cell monitoring. *ACS Omega*, 3(7), 7424–7431.

- Deschrevel, B., Tranchepain, F., & Vincent, J.-C. (2008). Chain-length dependence of the kinetics of the hyaluronan hydrolysis catalyzed by bovine testicular hyaluronidase. *Matrix Biology*, 27(5), 475–486.
- Fallacara, A., Baldini, E., Manfredini, S., & Vertuani, S. (2018). Hyaluronic acid in the third millennium. *Polymers*, 10(7), 701.
- Feng, Q., Lin, S., Zhang, K., Dong, C., Wu, T., Huang, H., Yan, X., Zhang, L., Li, G., & Bian, L. (2017). Sulfated hyaluronic acid hydrogels with retarded degradation and enhanced growth factor retention promote hMSC chondrogenesis and articular cartilage integrity with reduced hypertrophy. *Acta Biomaterialia*, 53, 329–342.
- Figueiredo, T., Jing, J., Jeacomine, I., Olsson, J., Gerfaud, T., Boiteau, J.-G., Rome, C., Harris, C., & Auzély-Velty, R. (2020). Injectable self-healing hydrogels based on boronate ester formation between hyaluronic acid partners modified with benzoxaborin derivatives and saccharides. *Biomacromolecules*, 21(1), 230–239.
- Gilbert, E. E. (1962). The reactions of sulfur trioxide, and its adducts, with organic compounds. *Chemical Reviews*, 62(6), 549–589.
- Gribkova, O. L., Iakobson, O. D., Nekrasov, A. A., Cabanova, V. A., Tverskoy, V. A., Tameev, A. R., & Vannikov, A. V. (2016). Ultraviolet-visible-near infrared and Raman spectroelectrochemistry of poly(3,4-ethylenedioxythiophene) complexes with sulfonated polyelectrolytes. The role of inter- and intra-molecular interactions in polyelectrolyte. *Electrochimica Acta*, 222, 409–420.
- Gribkova, O. L., Iakobson, O. D., Nekrasov, A. A., Cabanova, V. A., Tverskoy, V. A., & Vannikov, A. V. (2016). The influence of polyacid nature on poly(3,4-ethylenedioxythiophene) electrochemistry and its spectroelectrochemical properties. *Journal of Solid State Electrochemistry*, 20(11), 2991–3001.
- Guo, B., & Ma, P. X. (2018). Conducting polymers for tissue engineering. *Biomacromolecules*, 19(6), 1764–1782.
- Harman, D. G., Gorkin, R., Stevens, L., Thompson, B., Wagner, K., Weng, B., Chung, J. H. Y., in het Panhuis, M., & Wallace, G. G. (2015). Poly(3,4-ethylenedioxythiophene):dextran sulfate (PEDOT:DS) – A highly processable conductive organic biopolymer. *Acta Biomaterialia*, 14, 33–42.
- Hintze, V., Moeller, S., Schnabelrauch, M., Bierbaum, S., Viola, M., Worch, H., & Scharnweber, D. (2009). Modifications of hyaluronan influence the interaction with human bone morphogenetic protein-4 (hBMP-4). *Biomacromolecules*, 10(12), 3290–3297.
- Hofmann, A. I., Katsigiannopoulos, D., Mumtaz, M., Petsagkourakis, I., Pecaustings, G., Fleury, G., Schatz, C., Pavlopoulou, E., Brochon, C., Hadziioannou, G., & Cloutet, E. (2017). How to choose polyelectrolytes for aqueous dispersions of conducting PEDOT complexes. *Macromolecules*, 50(5), 1959–1969.
- Horikawa, M., Fujiki, T., Shiroaki, T., Ryu, N., Sakurai, H., Nagaoka, S., & Ihara, H. (2015). The development of a highly conductive PEDOT system by doping with partially crystalline sulfated cellulose and its electric conductivity. *Journal of Materials Chemistry C*, 3(34), 8881–8887.
- Kayser, L. V., & Lipomi, D. J. (2019). Stretchable conductive polymers and composites based on PEDOT and PEDOT:PSS. *Advanced Materials*, 31(10), 1806133.
- Kiristi, M., Oksuz, A. U., Oksuz, L., & Ulusoy, S. (2013). Electrospun chitosan/PEDOT nanofibers. *Materials Science and Engineering: C*, 33(7), 3845–3850.
- Kunze, R., Rösler, M., Möller, S., Schnabelrauch, M., Riemer, T., Hempel, U., & Dieter, P. (2010). Sulfated hyaluronan derivatives reduce the proliferation rate of primary rat calvarial osteoblasts. *Glycoconjugate Journal*, 27(1), 151–158.
- Liu, Y., Pharr, M., & Salvatore, G. A. (2017). Lab-on-skin: A review of flexible and stretchable electronics for wearable health monitoring. *ACS Nano*, 11(10), 9614–9635.
- Mantione, D., del Agua, I., Schaafsma, W., Diez-Garcia, J., Castro, B., Sardon, H., & Mecerreyes, D. (2016). Poly(3,4-ethylenedioxythiophene):GlycosAminoGlycan aqueous dispersions: Toward electrically conductive bioactive materials for neural interfaces. *Macromolecular Bioscience*, 16(8), 1227–1238.
- Mire, C. A., Agrawal, A., Wallace, G. G., Calvert, P., & in het Panhuis, M. (2011). Inkjet and extrusion printing of conducting poly(3,4-ethylenedioxythiophene) tracks on and embedded in biopolymer materials. *Journal of Materials Chemistry*, 21(8), 2671–2678.
- Möller, S., Schmidtke, M., Weiss, D., Schiller, J., Pawlik, K., Wutzler, P., & Schnabelrauch, M. (2012). Synthesis and antihypertensive activity of carboxymethylated and sulfated hyaluronan derivatives. *Carbohydrate Polymers*, 90(1), 608–615.
- Purcell, B. P., Kim, I. L., Chuo, V., Guenin, T., Dorsey, S. M., & Burdick, J. A. (2014). Incorporation of sulfated hyaluronic acid macromers into degradable hydrogel scaffolds for sustained molecule delivery. *Biomaterials Science*, 2(5), 693–702.

- Someya, T., Bao, Z., & Malliaras, G. G. (2016). The rise of plastic bioelectronics. *Nature*, *540*(7633), 379–385.
- Takano, T., Masunaga, H., Fujiwara, A., Okuzaki, H., & Sasaki, T. (2012). PEDOT nanocrystal in highly conductive PEDOT:PSS polymer films. *Macromolecules*, *45*(9), 3859–3865.
- Tekoglu, S., Wielend, D., Scharber, M. C., Sariciftci, N. S., & Yumusak, C. (2020). Conducting polymer-based biocomposites using deoxyribonucleic acid (DNA) as counterion. *Advanced Materials Technologies*, *5*(3), Article 1900699.
- Wang, S., Guan, S., Wang, J., Liu, H., Liu, T., Ma, X., & Cui, Z. (2017). Fabrication and characterization of conductive poly (3,4-ethylenedioxythiophene) doped with hyaluronic acid/poly (l-lactic acid) composite film for biomedical application. *Journal of Bioscience and Bioengineering*, *123*(1), 116–125.
- Wang, S., Oh, J. Y., Xu, J., Tran, H., & Bao, Z. (2018). Skin-inspired electronics: An emerging paradigm. *Accounts of Chemical Research*, *51*(5), 1033–1045.
- Xu, Y., Cui, M., Patsis, P. A., Günther, M., Yang, X., Eckert, K., & Zhang, Y. (2019). Reversibly assembled electroconductive hydrogel via a host-guest interaction for 3D cell culture. *ACS Applied Materials & Interfaces*, *11*(8), 7715–7724.
- Xu, Y., Patsis, P. A., Hauser, S., Voigt, D., Rothe, R., Günther, M., Cui, M., Yang, X., Wieduwild, R., Eckert, K., Neinhuis, C., Akbar, T. F., Minev, I. R., Pietzsch, J., & Zhang, Y. (2019). Cytocompatible, injectable, and electroconductive soft adhesives with hybrid covalent/noncovalent dynamic network. *Advanced Science*, *6*(15), Article 1802077.
- Yang, B., Yao, F., Ye, L., Hao, T., Zhang, Y., Zhang, L., Dong, D., Fang, W., Wang, Y., Zhang, X., Wang, C., & Li, J. (2020). A conductive PEDOT/alginate porous scaffold as a platform to modulate the biological behaviors of brown adipose-derived stem cells. *Biomaterials Science*, *8*(11), 3173–3185.
- Zozoulenko, I., Franco-Gonzalez, J. F., Gueskine, V., Mehandzhyski, A., Modarresi, M., Rolland, N., & Tybrandt, K. (2021). Electronic, optical, morphological, transport, and electrochemical properties of PEDOT: A theoretical perspective. *Macromolecules*, *54*(13), 5915–5934.